LBL-18315
CONF-8409144-2

Lawrence Berkeley Laboratory
UNIVERSITY OF CALIFORNIA

Accelerator & Fusion
Research Division

Presented at the 1984 Free Electron Laser Conference,
Castelgandolfo, Italy, September 1984

A STORAGE-RING FEL FOR THE VUV

J.M. Peterson, J.J. Bisognano, A.A. Garren,
K. Halbach, K.J. Kim, and R.C. Sah

September 1984

Prepared for the U.S. Department of Energy under Contract DE-AC03-76SF00098

LBL--18315

DE85 001646

Contributed Paper to the 1984 Free Electron Laser Conference

Castelgandolfo, Italy

Sept 1984

A Storage-Ring FEL for the VUV*

J.M. Peterson
J.J. Bisognano
A.A. Garren
K. Halbach
K.J. Kim
R.C. Sah

Lawrence Berkeley Laboratory
University of California
Berkeley, California, 94720
U.S.A.

* This work was supported by the Director, Office of Energy Research, Office of High Energy and Nuclear Physics, High Energy Physics Division, U.S. Dept. of Energy, under Contract No. De-Ac03-76SF00098.

LBL-18315

A Storage-Ring FEL for the VUV*

J.M. Peterson, J.J. Bisognano, A.A. Garren,
K. Halbach, K.J. Kim, R.C. Sah

Lawrence Berkeley Laboratory
University of California
Berkeley, California, 94720
U.S.A.

I. Summary

A free-electron laser for the VUV operating in a storage ring requires an electron beam of high density and low energy spread and a short wavelength, narrow-gap undulator. These conditions tend to produce longitudinal and transverse beam instabilities, excessive beam growth through multiple intra-beam scattering, and a short gas-scattering lifetime. Passing the beam only occasionally through the undulator in a by-pass straight section, as proposed by Murphy and Pellegrini [1], allows operation in a high-gain, single-pass mode and a long gas-scattering lifetime. Several storage ring designs have been considered to see how best to satisfy the several requirements. Each features a by-pass, a low-emittance lattice, and built-in wigglers for enhanced damping to counteract the intra-beam scattering.

II. Introduction

The use of a "single pass", high-gain free-electron laser in a by-pass straight section of an electron storage ring has the potential of providing

---

* This work was supported by the Director, Office of Energy Research, Office of High Energy and Nuclear Physics, High Energy Physics Division, U.S. Dept. of Energy, under Contract No. De-AcO3-76SF00098.

coherent radiation in the VUV region with peak power on the order of tens of megawatts. Locating the FEL in a by-pass, rather than in the storage ring proper, and switching the electron beam through it only about once per damping period, has two principal advantages: It allows the use of a narrow-gap undulator without causing an unacceptabley low gas-scattering lifetime, and it allows the disruptive effects on the elctron beam produced in the high-gain FEL to be damped out in the storage ring between FEL passages, thus minimizing the effective beam emittance and maximizing the gain in the FEL.

We have considered the problem of optimizing the parameters of such a system and are reporting the progress made to date.

III. Design of the Storage Ring System

Operation of free-electron lasers in the single-pass, high-gain mode requires both high density (large peak current and small emittance) and low momentum spread. These conditions place severe demands on storage ring performance, which is limited by both coherent and incoherent multiparticle phenomena. The longitudinal microwave instability causes growth of momentum spread as peak bunch current is increased, and maximum current can also be limited by single-bunch transverse fast blow-up. Multiple intra-beam scattering can cause emittance to grow well above the natural quantum-excitation value, and single, large-angle scattering (Touschek effect) can limit beam lifetimes. The large RF systems, which are required for good Touschek lifetimes and short bunch lengths, introduce substantial impedance into the storage ring. In addition, for smooth, low-impedance beam environments, the free-space impedance at microwave frequencies is not negligible.

The heart of the matter is that the operation of a free-electron laser in the high-gain mode is essentially a controlled instability, so that beam

parameters which insure good FEL performance also make the stored beam susceptible to a variety of other instabilities. The solution to this dilemma lies on the design of the storage ring to alleviate these current limitations. . Trade-offs with regard to lattice functions, synchrotron damping, RF voltages, machine radius, energy, and natural emittances can substantially improve performance.

We chose to examine two ring sizes and two beam energies and to judge these four cases on the basis of FEL performance as calculated using the FRED [2] computer program at the Lawrence Livermore National Laboratory. The storage rings considered are shown in Figures 1 and 2.

The basic lattice in each case consists of 6 achromatic sections of the Chasman-Green [3] type interspersed with three 10-meter straight sections and three damping-wiggler straight sections. Each ring has a by-pass with a 20-meter straight section for the single-pass, high-gain free-electron laser. The lattice wigglers were inserted to enhance the damping rate and thus limit the emittance growth due to multiple intra-beam scattering, as will be discussed. The 10-meter straight sections provide room for the injection system, the by-pass switches, the RF cavities, and also are available for various insertion devices.

The problem of designing suitable lattices requires obtaining low natural emittance, high momentum compaction and short damping time. The low emittance is obtained by having a sufficiently large number of achromats, in this case six. High momentum compaction, needed for longitudinal stability with small energy spread, is obtained by using long, low-field bending magnets. Since these magnets, unfortunately, produce only weak damping, it is necessary to introduce six high-field damping wigglers into the lattice.

The larger ring (150-meter circumference) has 16 quadrupoles per achromatic section and thus could be more fully optimized than the smaller ring (96-meter circumference), which has only 12 quadrupoles per achromat. The smaller ring represents an effort to mimimize the circumference.

The principal parameters of the four cases are listed in Table 1. The optics of the 500-MeV and 750-MeV versions of each ring differ principally because in each case the wiggler peak magnetic field was set at 1.8 telsa. Mechanically the rings are very close. The lattice functions for cases A and B are illustrated in Figure 3.

IV. High Intensity Effects

Since good FEL operation is based on a controlled beam instability, it is not surprising that other, more deleterious high-intensity effects can also occur in this high-beam-density domain. The most serious of these effects are the longitudinal and transverse coherent instabilities and multiple intra-beam scattering.

A. Coherent Beam Instabilities and Impedance

The threshold peak current for the longitudinal microwave instability is given by:

$$I_p^L = \frac{2\pi\alpha\,(E/e)\sigma_p^{\,2}}{Z_n/n} \qquad \text{(amperes)} \qquad (1)$$

where α is the momentum compaction factor, E is the beam energy (in eV), σ_p is the rms fractional momentum spread, and Z_n is the longitudinal coupling impedance (ohms) at the nth harmonic, here evaluated at the frequency $\omega = \sigma_s/c$ for the rms bunch length σ_s.

The threshold for the transverse instability is:

$$I_p^L = \frac{4\pi\sqrt{2}E\upsilon_s}{eZ_t\bar{\beta}} F(b/\sigma_s) \qquad (2)$$

where υ_s is the synchrotron tune, Z_t is the effective transverse impedance, $\bar{\beta}$ is the average value of the beta function in the transverse plane under consideration, b is the radius of the vacuum pipe, and F is a form factor of the order of unity.

For the examples considered here, the longitudinal instability produces the more stringent limit. We note that a larger compaction factor provides a larger longitudinal threshold. However it will develop that a larger compaction factor tends also to produce a larger emittance growth from multiple intra-beam scattering. Thus the choice of optimum compaction factor is somewhat complicated.

The sources of longitudinal coupling impedance include beam-pipe discontinuities, the RF cavities, and the free-space impedance at frequencies well above the beam-pipe cut-off. For this study 1 ohm was allotted for vacuum chamber discontinuities. An additional 1 to 3 ohms was introduced in the peak Z_n/n by the RF system, which was sized to produce a momentum dynamic aperture of ±3 percent, so as to provide an adequate lifetime for large-angle intra-beam scattering (Touschek effect).

From experience at SPEAR it is expected that above the pipe cut-off Z_n/n will fall as $(\omega_c/\omega)^{1.7}$. From this scaling, at frequencies corresponding to a bunch length of about 1 cm, the effective Z_n/n is less than 1 ohm for the combination of vacuum-chamber discontinuities and RF system.

The peak value of the free space impedance is given by the approximate relation:

$$\left(\frac{Zn}{n}\right)_{freespace} = 300\frac{b}{R} \text{ ohms} \qquad (3)$$

This value of impedance appears at frequencies well above pipe cut-off, where shielding of the synchrotron radiation process disappears.

If wigglers are introduced for enhanced synchrotron-radiation damping, there is an additional contribution proportional to the total additional absolute angular bend in the wigglers. Values in the 1 ohm range were obtained for the smaller rings considered.

8. Multiple Intra-Beam Scattering

Multiple Coulomb scattering between electrons within a bunch can lead to excitation of betatron oscillations and energy spread. If the synchrotron damping is weak compared with the diffusion rate induced by this intra-beam scattering, the equilibrium beam emittance can be substantially larger than the natural quantum emittance.

The theory of intra-beam scattering has been developed most fully in the work of Piwinski [4] and that of Bjorken and Mtingwa [5]. The detailed formulation requires numerical evaluation of rather involved expressions for transverse and longitudinal diffusion rates. The basic mechanism can be summarized as follows: In a typical intra-beam scattering event some transverse momentum is converted to longitudinal. This increase in longitudinal momentum coupled with the local dispersion function can increase the horizontal emittance in the same way that it tends to be increased by quantum excitation.

For electron storage rings of interest here there is growth in both longitudinal and horizontal emittance, and the primary scattering is from horizontal into longitudinal. An equilibrium emittance is reached when the intra-beam and quantum-exitation diffusion rates are balanced by the horizontal synchrotron damping. This condition is summarized by:

$$-g\epsilon_H + g\epsilon_o + G(\epsilon_H)\epsilon_H = 0 \qquad (4)$$

where g is the synchrotron damping rate, ϵ_H is the horizontal emittance, ϵ_o is the nominal quantum-exitation emittance, and $G(\epsilon_H)$ is the intra-beam-scattering diffusion rate, which is a complicated function of ϵ_H. In the parameter regime of interest, however, it is found that $G(\epsilon_H)$ is proportional to $(\epsilon_H)^{-2}$. Let $\hat{\epsilon}$ be the value of ϵ_H where $G(\hat{\epsilon})$ equals g -- that is, where the synchrotron damping equals the intra-beam diffusion rate. Then it follows from equation (4) that the equilibrium ϵ_H is given by:

$$\epsilon_H = \frac{1}{2}\left[\epsilon_o + (\epsilon_o + 4\,\hat{\epsilon}^2)^{1/2}\right] \qquad (5)$$

The scaling of this equilibrium emittance is not clear cut because the basic relations are not simple functions. It has been found useful to vary the relevant parameters in numerical evaluations to yield local behavior. For the lattices considered in this study, it was found that the growth rate of the horizontal emittance was proportional to the average value of the quantity

$$\left\langle \frac{I_p \tilde{D}}{\epsilon^2 \beta_y^{1/3} \sigma_p \gamma^3} \right\rangle \qquad (6)$$

where I_p is the peak beam current, $\tilde{D}^2 = D^2 + (\alpha D + \beta D')^2$, D being the dispersion

function, D' its slope, α and β the usual horizontal betatron functions, β_y the vertical betatron function, σ_p the rms fractional momentum spread, and γ the electron energy in units of the electron rest mass.

Using this proportionality, equation (5) can be rewritten as

$$\epsilon_H = \frac{1}{2}\left[\epsilon_o + \left[\epsilon_o^2 + (\text{const})\left(\frac{I_p \tilde{D} \mathcal{T}_s}{\beta_y^{1/3} \sigma_p \gamma^3}\right)\right]^{1/2}\right] \qquad (7)$$

where $\mathcal{T}_s$ is the synchrotron damping time. The constant is determined by the numerical evaluation of a particular case. Thus from an intra-beam-scattering point of view, design goals include: small natural emittance, small dispersion, small damping time, large β_y in the dispersion region, large σ_p, and high energy. Unfortunately, not all these conditions are consistent with other storage-ring current limitations or with optimum FEL performance. In particular, as was noted earlier, smaller dispersion results in a smaller compaction factor, which reduces the microwave instability threshold.

IV. Operating Conditions

Choice of the optimum operating conditions of a storage ring for FEL operation is complicated by the interdependence of the operating parameters at high beam intensities. Larger momentum spread allows larger currents through the microwave instability but tends to degrade FEL performance. Larger currents tend to produce larger emittance through intra-beam scattering, so that whether the current density also increases is not immediately apparent.

Our first step toward finding the optimum ring and its optimum operating conditions has been to consider for each ring two energies (500 and 750 MeV), two values of momentum spread (.001 and .002), and two values of vertical-to-horizontal emittance coupling ratio (1/10 and 1/1)-- a total of 16 cases. From these parameters are derived the corresponding values of maximum beam

current, emittance, and RF voltage. Table 2 shows the operating conditions for 8 of the cases considered.

V. FEL Performance

The FEL performance for each of the 16 cases was judged both by analytical expressions derived from theory [1,6-14] and by the results of the two-dimensional simulation code FRED.

One-dimensional theory predicts exponential growth and a saturation power level. The e-folding length for growth of the radiation power is

$$l_e = \frac{\lambda_w}{8\pi\rho\, f(\sigma_p/p)} \qquad (8)$$

where λ_w is the wiggler period, ρ is the FEL gain parameter, which for a planar undulator is approximately

$$\rho = \left\{\frac{K^2}{16\pi}[J_0(\mu) - J_1(\mu)]^2 \lambda_w^2 n_e r_e / \gamma^3\right\}^{1/3} \qquad (9)$$

where K is the rms undulator parameter = $0.934\lambda_w(\text{cm})B(T)$, B the rms wiggler field strength, n_e the volume density of the electron beam, r_e the classical electron radius, $\mu = K^2/(1 + K^2)$, and $f(\sigma_p/\rho)$ is a function of the electron fractional energy spread in units of ρ; the value f(0) is 0.866, and f(1) is 0.31 for a Lorentzian momentum distribution. Note that equations (8) and (9) are generalized relative to those of reference [1] in that they apply to a planar undulator and include the effects of momentum spread.

B for a hybrid wiggler using samarium-cobalt permanent magnets (B_r = 0.9 Telsa) is approximately [15]

$$B = 2.36\, e^{-g/\lambda_w}(5.47 - 1.8g/\lambda_w) \quad \text{(Tesla)} \qquad (10)$$

where g is the wiggler full gap. The wiggler period and the radiation wave length λ are related by the resonance condition

$$\lambda = \frac{\lambda_w}{2\gamma^2}(1 + K^2) \qquad (11)$$

The exponential growth of the radiation field eventually levels off. The saturation level is expected to be of the order of ρE_b, E_b being the power in the electron beam. Note that the value ρE_b is only a crude estimate of the saturation level in that it contains no allowance for the effects of energy spread in the electron beam. 1-D numerical examples [1] have shown substantial reduction in the saturation level when the energy spread σ_p is of the order of or greater than ρ. The number of undulator periods need to reach saturation is expected to be about $1/\rho$; thus the undulator length required to reach saturation is approximately λ_w/ρ.

The FEL parameters and estimated operating levels are listed in Table 2. Comparison of these operating levels with those computed by the two-dimensional simulation code FRED has started but as yet is far from complete. The preliminary results seem to indicate qualitative agreement -- i.e., the cases which look better on the basis of analytic expressions also look better according to FRED. Quantitatively, the results at present are not conclusive The exponentiating length according to FRED is typically about 50 percent longer than the analytic estimate, and the saturating power level is typically an order of magnitude lower than ρE_b. The systematics of the quantitative differences are not yet understood, but there are indications that diffraction effects are at least partly responsible. Also it seems likely that the effects of energy spread will help explain the difference between the saturation power levels calculated by FRED and the values of ρE_b.

VI. Conclusions

In comparing the various rings and operating conditions, the present results indicate that the 150-meter ring operating at 750 MeV with a σ_p of .002 and an emittance-coupling ratio of 0.1 is the best of the 16 cases considered. Whether a larger radius ring is inherently better is, however, not yet clear, because in the light of these studies we can now see the possibility that the lattice of the smaller ring could be significantly improved with respect to both natural emittance and intra-beam scattering.

The power levels available from a high-gain FEL may not be as high as anticipated on the basis of analytic theory, but nevertheless the computational results indicate that powers on the order of tens of megawatts can be obtained in systems like those considered in this report.

Table 1

The Principal Lattice Parameters of the Four Rings Considered

CASE	A	B	C	D
Circumference, m	150	96	150	96
Beam energy, MeV	500	500	750	750
Superperiods	3	3	3	3
Insertion SS, m	10	10	10	10
Wiggler SS, m	9	5.4	9	5.4
Bend field, T	0.218	0.647	0.327	0.873
Wiggler field, T	1.8	1.8	1.8	1.8
Wiggler length, m	3 x 7.8	3 x 4.2	3 x 7.8	3 x 4.2
Wiggler period, m	0.3	0.3	0.3	0.3
Betatron tunes, x/y	6.68/7.72	5.31/5.27	6.63/6.60	6.69/3.44
β in SS, x/y, m	2.8/5.0	10/3.2	3.2/4.6	3.0/7.0
Chromaticity x/y	15.0/17.7	11.0/10.6	13.7/12.0	23.5/7.1
Compaction factor α	.0166	.0074	.0167	.0084
τ_x without wigglers, sec.	0.69	.15	.21	.05
τ_x with wigglers, sec.	0.030	.030	.019	.016
ϵ_{xo}, natural, 10^{-8} rad-m	0.246	0.654	0.324	0.834
σ_p, natural, without wigglers, 10^{-4}	1.55	2.67	2.33	3.80
σ_p, natural, with wigglers, 10^{-4}	4.36	4.16	5.24	4.97

Table 2

8 Sets of Operating Conditions

Ring circumference, m	150	96	150	96	150	96	150	96
Beam Energy, MeV	500	500	750	750	500	500	750	750
Momentum spread σ_p	.001	.001	.001	.001	.002	.002	.002	.002
ϵ_y/ϵ_x	0.1	0.1	0.1	0.1	0.1	0.1	0.1	0.1
ϵ_x, 10^{-8} rad-m	1.23	0.98	0.71	0.84	1.74	1.27	0.96	0.93
σ_s, cm	1.25	1.25	1.25	1.25	1.25	1.25	1.25	1.25
Peak current, amp	74	23	82	46	296	93	327	183
$RF_{voltage}$, MV	3.0	0.86	4.5	1.5	3.0	0.86	4.5	1.5
FEL parameters:								
λ, A°	400	400	400	400	400	400	400	400
λ_w, cm	1.88	1.88	2.34	2.34	1.88	1.88	2.34	2.34
K (rms)	1.80	1.80	2.58	2.58	1.80	1.80	2.58	2.58
Gain parameter, ρ, 10^{-3}	1.00	0.74	1.09	0.85	1.43	1.08	1.56	1.30
ρE_b, MW	37	8.5	67	29	211	50	382	178
λ_w/ρ, m	18.7	25.5	21.6	27.6	13.2	17.4	15.0	18.0

REFERENCES

[1] J.B. Murphy and C. Pellegrini, "Generation of High Intensity Coherent Radiation in the Soft X-Ray and VUV Region", BNL unpublished, 1984.

[2] Access to the FRED program was generously provided by Andrew Sessler, Donald Prosnitz, and Ernst T. Scharlemann.

[3] R. Chasman and G.K. Green, BNL 50595 (J.P. Blewett editor), Vol. 1, pp 4-4 to 4-8, 1977.

[4] Piwinski, "Intra-Beam Scattering", IXth International Conference on High Energy Accelerators, SLAC, 1974.

[5] J. Bjorken and S. Mtingwa, "Intra-Beam Scattering", Particle Accelerators, 13, 115, 1983.

[6] R. Bonifacio, L. Narducci, and C. Pellegrini, "Proc. of Topical Meeting on Free Electron Generation of Extreme UV Coherent Radiation, BNL, Sept 1983, AIP Conf. Proc. No. 118, Subseries on Optical and Engineering No. 4, 1984.

[7] N.M. Kroll and W.A. McMullin, Phys. Rev. A17, 300 (1978)

[8] A. Gover and Z. Livni, Opt. Comm. 26, 375 (1978).

[9] I.B. Bernstein and J.L. Hirshfeld , Phys. Rev. A20, 1661 (1979).

[10] C.C. Shil and A. Yariv, IEEE J. of Quantum Electron., QE-17 1387 (1981).

[11] P. Sprangle, C.M. Tang and W.M. Manheimer, Phys. Rev. A20, 302, (1980).

[12] G. Dattoli, A. Marino, A. Renieri, F. Romanelli, IEEE J. of Quantum Electron. , QE-17, 1371 (1981).

[13] A. Gover, P Sprangle, IEEE J. of Quantum Electron. , QE-17, 1196 (1981).

[14] R. Bonifacio, F. Casagrande and G. Casati, Opt. Comm. 40, 219 (1982).

[15] K. Halbach, Journal de Physique Collogue C1-211, Tome 44 (1983)

List of Figures

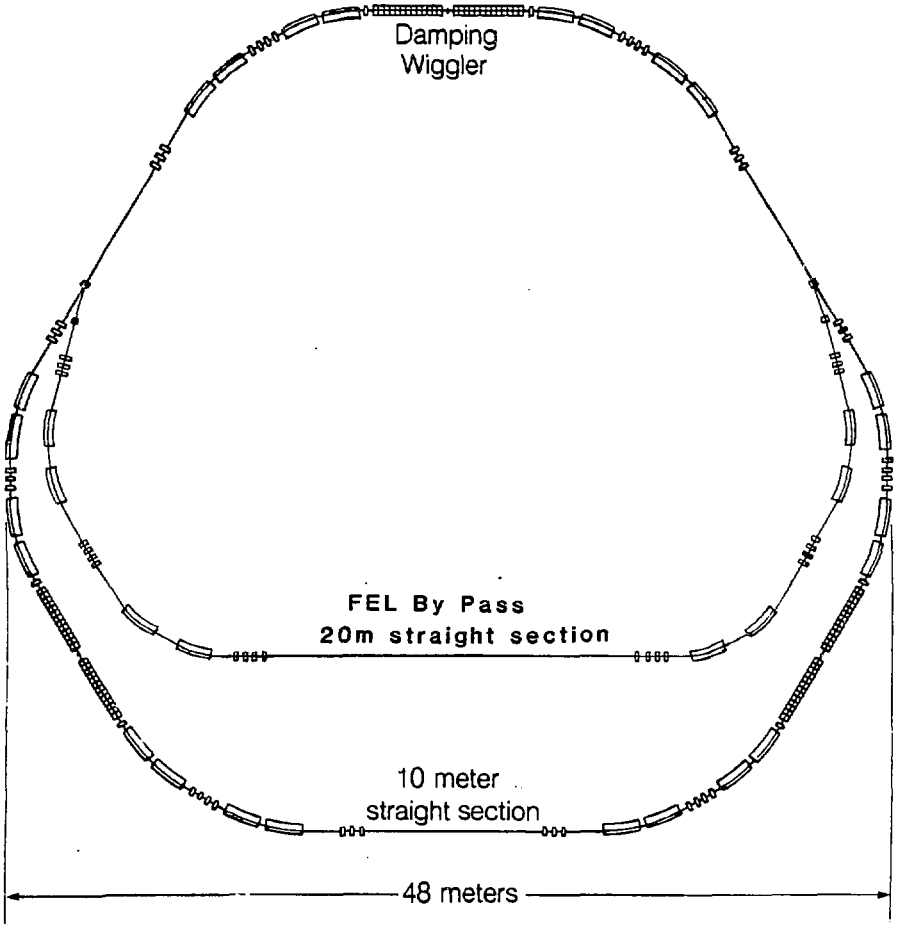

Figure 1 150 meter Circumference Storage Ring with FEL By-Pass

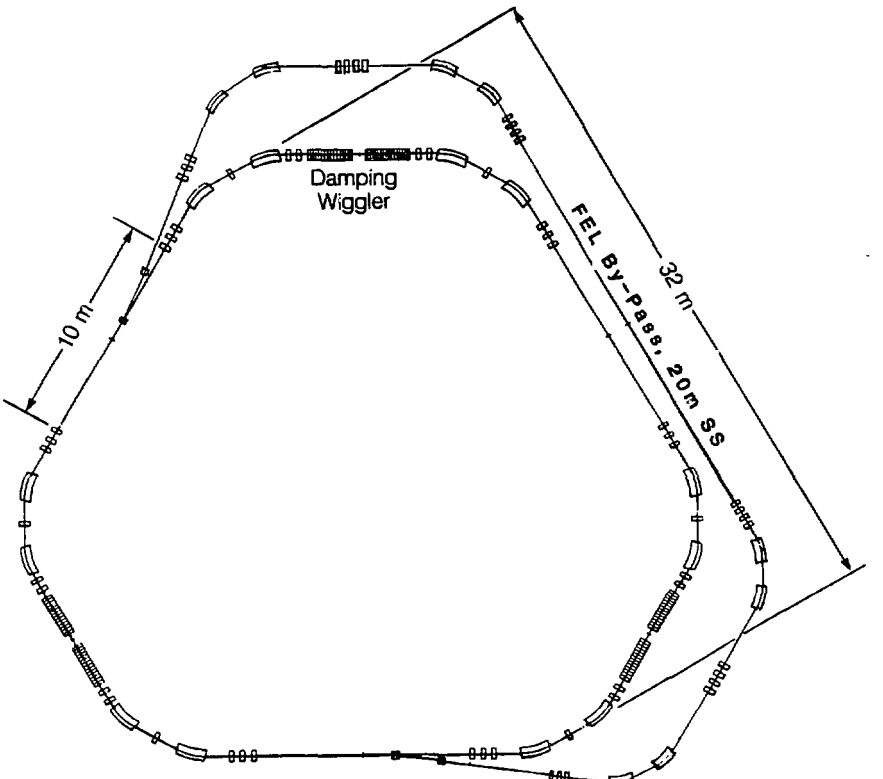

Figure 2 96 meter Circumference Storage Ring with FEL By-Pass

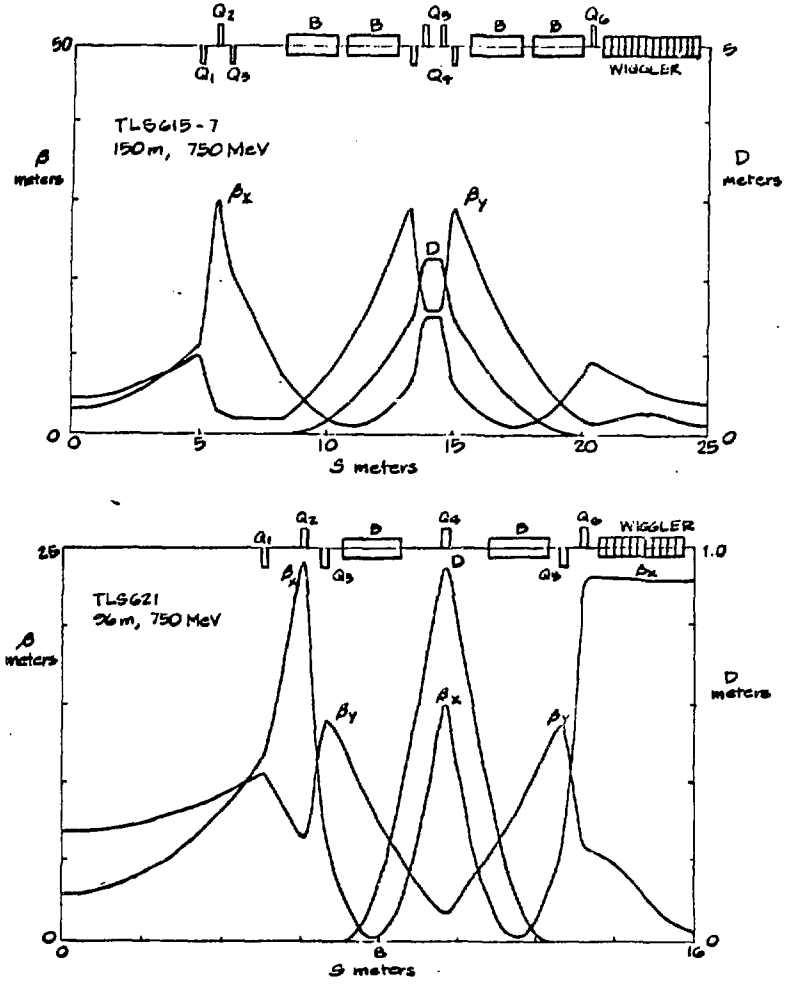

Figure 3 The betaron and disperion functions for the 150-meter and the 96-meter lattices at 750 MeV.